analytical chemistry

Article

pubs.acs.org/ac

A Highly Selective and Instantaneous Nanoprobe for Detection and Imaging of Ascorbic Acid in Living Cells and in Vivo

Na Li, Yanhua Li, Yaoyao Han, Wei Pan, Tingting Zhang, and Bo Tang*

College of Chemistry, Chemical Engineering and Materials Science, Collaborative Innovation Center of Functionalized Probes for Chemical Imaging, Key Laboratory of Molecular and Nano Probes, Ministry of Education, Shandong Normal University, Jinan 250014, People's Republic of China

Supporting Information

ABSTRACT: The development of a specific reaction of nanomaterials and reactive species is of fundamental importance for the determination of biomolecules. Here we report a novel nanoprobe for detection and imaging of ascorbic acid (AA) in living cells and in vivo based on the specific reaction of cobalt oxyhydroxide (CoOOH) and AA. Persistent luminescence nanoparticles (PLNPs) were used as the luminescence unit, and CoOOH nanoflakes served as the quencher. When CoOOH was modified on the surface of the PLNPs, the luminescence of the PLNPs was efficiently quenched by the CoOOH. In the presence of AA, CoOOH was reduced to Co^{2+} and the luminescence of PLNPs was restored. The nanoprobe showed high selectivity and an instantaneous response. The luminescence property permits detection and imaging without external excitation, which could effectively avoid background noise and scattering of light from biological matrixes produced by in situ excitation. The current strategy provides an effective platform for monitoring and imaging reactive species in living cells and in vivo.

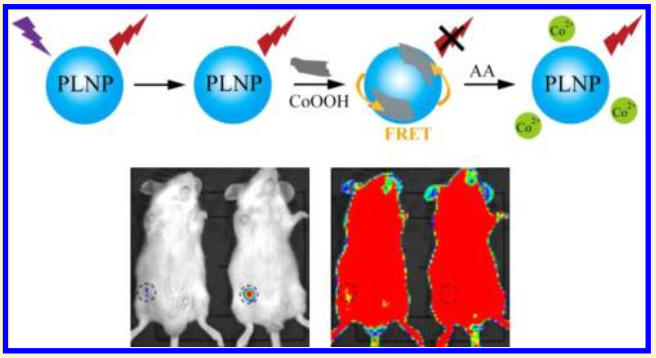

Small-molecule reactive species play crucial roles in cell signaling and thus are involved in both human health and disease.[1−3] Consequently, the detection of these biomolecules is of great importance in living cells and in vivo. Among the detection techniques, fluorescence analysis offers new opportunities for determination and imaging at the cellular level due to its simplicity and low detection limit.[4−6] In recent years, many organic fluorescent probes have been exploited for detection and imaging of reactive species in living cells or in vivo.[7−9] However, some drawbacks are unavoidable for most of these organic fluorophores, such as difficult separation, easy photobleaching, and poor photostability.[10,11] To address these issues, a new method was introduced to detect and image intracellular reactive species using nanoparticles (NPs), based on the specific reaction of nanomaterials and reactive species. Liu and co-workers described a method based on the specific reaction of MnO_2 and glutathione (GSH) for rapid and selective detection of GSH in living cells.[12] He et al. reported a nanoprobe based on the reaction of Ag and H_2S for selective and sensitive detection and imaging of H_2S in live cells using gold nanorod−silver core−shell NPs.[13] Despite these examples, the development of a specific reaction between the nanomaterials and reactive species is still at a preliminary stage. Taking into account the concept and the significance of detecting reactive species, we discovered that cobalt oxyhydroxide (CoOOH) nanoflakes could specifically react with ascorbic acid (AA) in an instantaneous manner. AA is an essential micronutrient required for numerous physiological and biochemical functions in the human body and is a potent water-soluble antioxidant capable of readily scavenging a number of reactive species and effectively protecting other biomolecules from oxidative damage.[14−16] The oxidative damage to lipids, DNA, and proteins has been implicated in many chronic diseases, such as cardiovascular disease, cancer, and cataracts. In addition, a variety of epidemiologic studies and clinical trials have shown that AA is associated with a reduction in the incidence of chronic disease and mortality.[17−19] Therefore, it is very significant to develop such a specific reaction for highly selective and rapid detection of AA.

In this study, we develop a novel nanoprobe for determination and screening of AA in living cells and in vivo using CoOOH-modified persistent luminescence nanoparticles (PLNPs). To the best of our knowledge, this is the first report that a nanoprobe was successfully applied for imaging reactive species in vivo without external excitation. CoOOH was employed as the recognition unit due to its specific reaction with AA. The PLNPs were employed as the luminescence unit, which can be optically excited with a UV lamp before analytical measurements.[20−23] Moreover, the persistent luminescence of PLNPs is still detectable after several hours, allowing the removal of the background noise produced by the in situ

Received: January 6, 2014
Accepted: March 21, 2014
Published: March 21, 2014

   dx.doi.org/10.1021/ac5000587 | *Anal. Chem.* 2014, 86, 3924−3930

excitation. Accordingly, the signal-to-noise ratio can be greatly increased when applied for detection in organisms and real-time imaging of reactive species. These characteristics make the PLNPs highly attractive as candidates for biological labeling and imaging in living cells and in vivo. Because the emission spectrum of the PLNPs overlaps with the absorption spectrum of CoOOH nanoflakes, the luminescence of the PLNPs can be efficiently quenched by CoOOH via Förster resonance energy transfer (FRET). In the presence of AA, the CoOOH nanoflakes on the surface of the PLNPs are reduced to Co^{2+} and the luminescence of PLNPs is restored with the relative amounts of AA. The details of this strategy are described in Scheme 1.

Scheme 1. Schematic Illustration of the Design for AA Detection Using CoOOH-Modified PLNPs

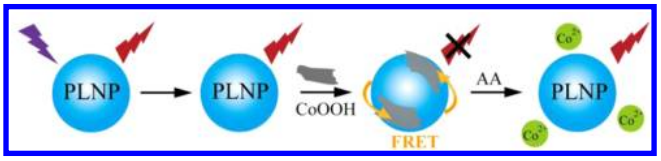

EXPERIMENTAL SECTION

Materials. Magnesium nitrate [$Mg(NO_3)_2{\cdot}6H_2O$] and cobaltous chloride ($CoCl_2{\cdot}6H_2O$) were purchased from Tianjin Guangfu Fine Chemical Research Institute (Tianjin, China). Strontium carbonate ($SrCO_3$)was purchased from Aladdin (Shanghai, China). Europium nitrate [$Eu(NO_3)_3{\cdot}6H_2O$] and dysprosium nitrate [$Dy(NO_3)_3{\cdot}5H_2O$] were purchased from Jinan Camolai Trading Co. (Jinan, China). Sodium hypochlorite (NaClO), sodium hydroxide (NaOH), ascorbic acid, tetraethoxysilane (TEOS), and the amino acids were from China National Pharmaceutical Group Corp. (Shanghai, China). 3-(4,5-Dimethylthiazol-2-yl)-2,5-diphenyltetrazolium bromide (MTT) was purchased from Sigma Chemical Co. RAW 264.7 macrophage cells were purchased from the Committee on Type Culture Collection of the Chinese Academy of Sciences. All the chemicals were analytical grade and used without further purification. Sartorius ultrapure water (18.2 MΩ cm) was used throughout the experiments.

Instruments. Transmission electron microscopy (TEM) was carried out on a JEM-100CX II electron microscope. The crystal structure of the samples was determined by powder X-ray diffraction (XRD) patterns (Bruker D8, Germany), using Cu Kα radiation (λ = 1.54178 Å) at a scanning rate of 0.02 deg s^{-1} in the 2θ range from 10° to 80°. Digital photographs were taken with a Nikon P5000 camera. X-ray photoelectron spectroscopy (XPS) was performed with a PHI 5300 ESCA system (Perkin-Elmer) equipped with five channeltrons using an unmonochromated Mg Kα X-ray source (1253.6 eV). Absorption spectra were measured on a pharmaspec UV-1700 UV−vis spectrophotometer (Shimadzu, Japan). Fourier transform infrared (FT-IR) spectra were obtained on a Varian 3100 FT-IR spectrometer. Fluorescence spectra were obtained with an FLS-920 Edinburgh fluorescence spectrometer and 1.0 cm quartz cells with slit widths of 15 nm and without in situ excitation. All pH measurements were performed with a pH-3c digital pH meter (Shanghai LeiCi Device Works, Shanghai, China) with a combined glass−calomel electrode. Absorbance was measured with a microplate reader (RT 6000, Rayto, United States) in the MTT assay. The fluorescence imaging studies were performed with a Leica DMI6000 fluorescence microscope (Leica Co., Ltd., Germany).

Synthesis of Persistent Luminescence Nanoparticles. The $Sr_2MgSi_2O_7$:1% Eu, 2% Dy PLNPs were synthesized using the typical sol−gel synthesis method reported previously with some modifications.[20] A 0.7382 g sample of $SrCO_3$ powder was dissolved in concentrated nitric acid under vigorous stirring to obtain a $Sr(NO_3)_2$ solution. $Mg(NO_3)_2{\cdot}6H_2O$ (0.6410 g), $Eu(NO_3)_3{\cdot}6H_2O$ (0.0335 g), and $Dy(NO_3)_3{\cdot}5H_2O$ (0.0658 g) were dissolved in ultrapure water to obtain a solution with a final volume of 10 mL after the addition of $Sr(NO_3)_2$ solution. Then the resulting solution was acidified to pH 2.0 by adding concentrated nitric acid. A 1.15 mL sample of TEOS was then added rapidly, and the solution was stirred at room temperature until it became transparent. The solution was heated at 70 °C until the sol-to-gel transition occurred. To obtain an opaque gel, the wet gel was then dried in an oven at 110 °C for 20 h. The resulting opaque dry gel was then fired at 1000 °C for 10 h in a zirconium crucible in a weak reductive atmosphere using 10% H_2, 90% Ar to obtain white crystals. Nanoparticles were obtained by basic wet grinding of the solid (500 mg) for 15 min with a mortar and pestle in a minimum volume of 5 mM NaOH solution. Hydroxylation was then performed overnight by dispersing the ground powder in 50 mL of the same NaOH solution to obtain hydroxylated PLNPs. After neutralization with HCl, the suspension was diluted with distilled water at a concentration of 2.5 mg/mL and gently centrifuged at 3000 rpm for 10 min to eliminate the largest particles. Acetone corresponding to 25% of the supernatant volume was added to promote sedimentation of the NPs. The suspension was then centrifuged at 10 000 rpm for 10 min to obtain the PLNPs.

Formation of CoOOH. A 100 μL sample of sodium hypochlorite (NaClO; 0.2 M) and 100 μL of sodium hydroxide (NaOH; 0.8 M) were added to 200 μL of $CoCl_2$ (10 mM) solution, and then the mixture was sonicated for 1 min. Subsequently, the product was collected by centrifugation, washed three times with deionized water, and dried in an oven. Then the product was characterized by XPS and FT-IR. The results revealed the formation of CoOOH according to previous reports.[24,25] The XPS result showed that the cobalt existed in the Co(III) oxidation state (780 eV) without any impurity of the Co(II) oxidation state[2] (Figure S2, Supporting Information). The FT-IR spectrum of CoOOH in the range of 4000−450 cm^{-1} is shown in Figure S3 (Supporting Information). The broad band at 3420 cm^{-1} is attributed to the bond stretching of the hydrogen-bonded hydroxyl group (−OH). The peak at 1630 cm^{-1} is characteristic of the Co−O double bond in the crystal structure of CoOOH, while the peak at about 600 cm^{-1} corresponds to the Co−O^{2-} complex in the oxide.

Preparation of CoOOH-Modified PLNPs. A 100 μL sample of the hydroxylated PLNPs (10 mg/mL) was added to a 2 mL microcentrifuge tube containing different amounts of $CoCl_2$ (10 mM, 0−200 μL). A 100 μL sample of NaClO (0.2 M) and 100 μL of NaOH (0.8 M) were then added to the tube. The resulting mixture was sonicated for 1 min. Subsequently, the CoOOH-modified PLNPs were collected by centrifugation, washed three times with deionized water, and redispersed in 1 mL of deionized water. The CoOOH-modified PLNPs were excited with a UV lamp for 10 min to obtain afterglow luminescence, which was then measured with the FLS-920 at 470 nm without in situ excitation. The photoluminescence (PL) intensity of the PLNPs decreased with increased

dx.doi.org/10.1021/ac5000587 | Anal. Chem. 2014, 86, 3924−3930

concentrations of $CoCl_2$ (Figure S9, Supporting Information). In the following experiments, the CoOOH-modified PLNPs (addition of 75 μL of $CoCl_2$) were chosen as an example.

Stability of the Nanoprobe. CoOOH-modified PLNPs were dispersed in 20 mM PBS buffer (1 mg/mL) with various pH values (6.8−8.3) and then excited with a UV lamp for 10 min to obtain afterglow fluorescence. After 45 min, the PL of the resulting solutions was measured at 470 nm without in situ excitation. CoOOH-modified PLNP aqueous solution (1 mg/mL) was excited with a UV lamp for 10 min. After 45 min, the PL of the CoOOH-modified PLNP solution was measured at 470 nm without in situ excitation at different temperatures (20, 25, 30, 35, and 40 °C). CoOOH-modified PLNPs (1 mg/mL) were dispersed in water and in different buffers (20 mM), including boric acid−borax saline (BBS) buffer, phosphate-buffered saline (PBS), 4-(2-hydroxyethyl)-1-piperazineethanesulfonic acid (HEPES), and 2-(*N*-morpholino)ethanesulfonic acid (MES). The PL of the resulting solutions was measured according to the method mentioned above.

Detection of Ascorbic Acid. Aliquots of 1.0 mL volume of freshly prepared CoOOH-modified PLNPs (1 mg/mL) were added to 2 mL microcentrifuge tubes, and then different concentrations (0, 1, 2, 4, 6, 10, 20, 30, 40, 50, 60, 70, 80, and 100 μM) of AA solution were added. The PL of the resulting solutions was measured immediately at 470 nm without in situ excitation.

Kinetics. CoOOH-modified PLNPs (the nanoprobe, 1 mg/mL) were excited with a UV lamp for 10 min to obtain afterglow fluorescence. After 45 min, certain amounts of AA solution (the final concentration of AA was 100 μM) were sequentially added at room temperature. Then the afterglow luminescence was measured immediately at 470 nm without in situ excitation for 30 s.

Verification of Reaction Products. To determine the products of the reaction of CoOOH and AA, one group of CoOOH-modified PLNPs (1 mg/mL) was treated with AA (the final concentration was 100 μM) and another group of CoOOH-modified PLNPs (1 mg/mL) was untreated. Then the two samples were centrifuged, and the supernatant was collected. UV−vis results showed an absorption peak of Co^{2+} appeared in the supernatant treated with AA, while there was no obvious absorption peak in the supernatant without AA (Figure S12, Supporting Information). The mass spectrum showed that dehydroascorbic acid (173.0073) was formed in the supernatant after the reaction (Figure S13, Supporting Information).

Selectivity of the Nanoprobe. The response of an interfering substance was measured by addition of interfering substances to a 2 mL nanoprobe solution (1 mg/mL). Taking the complex intracellular environment into consideration, the interfering substances were selected for mainly organism amino acids and small molecules and metal ions with physiological concentrations: AA (100 μM), Fe^{3+} (0.36 mM), Fe^{2+} (10 μM), Al^{3+}, Mg^{2+}, Na^+, and Zn^{2+} (0.18 mM), Cu^{2+}, K^+, and Ca^{2+} (0.12 mM), Cd^{2+} (36 μM), Co^{2+} (0.36 mM), NaClO (1.2 mM), H_2O_2 (10 μM), t-BuOOH and hydroquinone (HQ) (36 μM), GSH (1 mM), L-Cys (100 μM), Tyr, L-Arg, Lys, Gly, Hcy, and Trp (10 μM), $NaHSO_3$ and NaH_2PO_2 (100 μM), $H_2C_2O_4$ and $NaNO_2$ (500 μM), $Na_2S_2O_3$ (1 mM).

Cell Culture. RAW 264.7 macrophage cells were cultured in Dulbecco's modified Eagle's medium (DMEM). All cell lines were supplemented with 10% fetal bovine serum and 100 U/mL 1% antibiotic penicillin/streptomycin and maintained at 37 °C in a 100% humidified atmosphere containing 5% CO_2.

Detection of AA in Cell Extracts. RAW 264.7 macrophage cells were cultured for 24 h and washed twice with PBS buffer. After 2 mL of PBS buffer was added, the cell suspension was transferred to a 4 mL microcentrifuge tube. These cells were sonicated for 10 min below 4 °C. The disrupted cell suspension was centrifuged (14 800 rpm) for 20 min, and the supernatant was collected. The fluorescence of cell extracts with AA (100 μM) was detected with an excitation wavelength of 365 nm. Then the sample was measured at 470 nm without in situ excitation. After that, the CoOOH-modified PLNPs (1 mg/mL) were dispersed in the cell extracts with AA (100 μM) at room temperature. The mixture was excited with a UV lamp for 10 min to obtain afterglow fluorescence. Then the mixture was measured with 365 nm excitation and without in situ excitation as mentioned above. The cell extracts with PLNPs (1 mg/mL, Figure 4C, bottle a) and CoOOH-modified PLNPs (1 mg/mL, Figure 4C, bottles b and c) were placed in three glass bottles. The three samples were all excited with a UV lamp for 10 min before photographs were taken using a camera in the dark. Then certain amounts of AA (the final concentration of AA was 100 μM) were sequentially added to bottle c. Photographs were acquired using a camera in the dark (Figure 4D). The detection range of the nanoprobe was investigated in the cell extracts. CoOOH-modified PLNPs were dispersed in the cell extracts (1 mg/mL), and then different concentrations (0, 2.5, 7.5, 25, 35, 50, 60, 75, and 100 μM) of AA solution were added. The PL intensity of the resulting solutions was measured immediately at 470 nm without in situ excitation.

Persistent Luminescence Imaging of AA in Living Cells. RAW 264.7 macrophage cells were plated on chamber slides for 24 h, and then the CoOOH-modified PLNPs (0.2 mg/mL) were delivered into the cells in DMEM culture medium at 37 °C in 5% CO_2. After 1 h of incubation of the CoOOH-modified PLNPs and the cells, the cells were washed twice with PBS buffer. Before imaging, the sample was excited under a UV lamp for 10 s. The PL images were observed quickly with a DMI 6000 fluorescence microscope. Then 100 μM AA was added to the above sample. The PL images were observed according to the above procedure.

MTT Assay. RAW 264.7 macrophage cells were cultured in 96-well microtiter plates and incubated at 37 °C in 5% CO_2 for 24 h. After the original medium was removed, the cells were incubated with CoOOH-modified PLNPs (0.1, 0.2, 0.5, 1, 1.5, and 2 mg/mL) for 1 h. Then the cells were washed with PBS three times. Next, 150 μL of MTT solution (0.5 mg/mL) was added to each well. After 4 h, the remaining MTT solution was removed, and 150 μL of DMSO was added to each well to dissolve the formazan crystals. The absorbance was measured at 490 nm with the RT 6000 microplate reader.

Persistent Luminescence Imaging of AA in Vivo. To demonstrate the applicability of the nanoprobe to monitor AA in vivo, animal imaging was conducted as follows. First, two Kunming mice were anesthetized using 4% chloral hydrate (250 μL). The living mice were injected intraperitoneally with 0.1 mL of normal saline (left mouse in both panels in Figure 6) or 0.1 mL of AA solution (0.1 mol/L, right mouse in both panels in Figure 6) and then injected with 0.1 mL of CoOOH-modified PLNPs (1 mg/mL, excited by a 365 nm UV lamp for 10 min before injection) separately. Then luminescence signals were collected by a Caliper IVIS Lumina III without excitation (Figure 6A) and with 420 nm excitation (Figure 6B).

dx.doi.org/10.1021/ac5000587 | *Anal. Chem.* 2014, 86, 3924−3930

RESULTS AND DISCUSSION

Preparation and Characterization of the Nanoprobe. The $Sr_2MgSi_2O_7$:Eu,Dy PLNPs were first prepared using a modified sol−gel approach according to the previous report[20] (Figure 1A; Figure S1, Supporting Information). The PL of the PLNPs lasted more than 200 min and became stable 55−200 min after excitation (Figure 1C,D). Then the surface of the PLNPs was modified with free hydroxyl groups, which gave the PLNPs a negative surface (ζ potential −36.5 mV). The negative surface of the PLNPs was beneficial to attract more Co^{2+} and assemble the nanoprobe. Next, the as-prepared hydroxylated PLNPs were used to direct the growth of the CoOOH by the addition of $CoCl_2$ solution in the presence of NaOH and NaClO. $CoCl_2$ was oxidized by NaClO to form amorphous CoOOH nanoflakes (the characterization of CoOOH formation is given in the Supporting Information, Figures S2 and S3). The assembly of the CoOOH/PLNP nanoprobe was confirmed by TEM (Figure 1B). Compositional analyses with XPS further indicated the presence of CoOOH in the hybrid nanoprobe (Figure S4, Supporting Information).

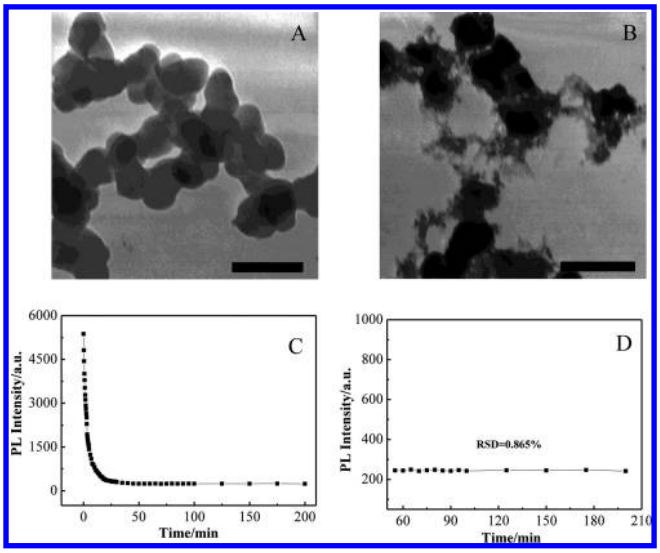

Figure 1. (A) TEM image of $Sr_2MgSi_2O_7$:Eu,Dy PLNPs. (B) TEM image of the CoOOH-modified PLNPs. Scale bars are 100 nm. (C) Time-dependent PL intensity of PLNPs (1 mg/mL) without further excitation after direct exposure under a UV lamp for 10 min. (D) Time-dependent PL intensity from 55 to 200 min of the PLNPs in (C).

Verification the Formation of the CoOOH-Modified PLNPs. The optical properties of the independent materials and the nanoprobe were evaluated. UV−vis absorption spectroscopy showed that the absorption peak of $CoCl_2$ was centered at 510 nm. When the CoOOH nanoflakes were formed, the absorption peak was blue-shifted to about 410 nm (Figure S5, Supporting Information). As can be seen from Figure S6 (Supporting Information), the absorption band of CoOOH nanoflakes overlaps with the emissions of the PLNPs, thereby enabling the generation of FRET. Figure S7 (Supporting Information) shows that the free PLNPs did not have obvious absorption, while the nanoprobe had an intense broad band centered at about 410 nm, which is consistent with the characteristic absorption of CoOOH, suggesting the successful modification of CoOOH on the surface of PLNPs. To further confirm the results, a physical mixture of preformed CoOOH nanoflakes and the PLNPs was prepared for comparison. As shown in Figure S8 (Supporting Information), the physical mixture did not lead to a significant change in PL intensity compared with free PLNPs, while the nanoprobe showed an obvious PL intensity decrease due to the FRET effect.

FRET of the Nanoprobe and the Response for AA. The energy transfer of the nanoprobe was confirmed by the observation of PL quenching of the PLNP solution upon modification of different ratios of CoOOH. Figure S9 (Supporting Information) indicates that the PL intensity decreased with an increase of the CoOOH concentration in the nanoprobe. The maximum quenching efficiency could reach as high as 93%. The stability of the nanoprobe was investigated in different media and at different pH values and temperatures. When the nanoprobe was in different pH conditions, the PL intensity showed a slight increase from pH 6.8 to pH 7.4, while the PL intensity was almost constant from pH 7.4 to pH 8.3, suggesting that the nanoprobe was basically stable in physiological pH conditions (Figure S10A, Supporting Information). Moreover, the PL intensity of the nanoprobe did not show an obvious change in different media (H_2O, BBS, PBS, HEPES, and MES) and at different temperatures (20, 25, 30, 35, and 40 °C) (Figure S10B,C). This demonstrated that the current nanoprobe was stable in different conditions. Addition of AA to CoOOH/PLNPs in aqueous solutions led to an obvious recovery of the emission of the nanoprobe, because of the separation of CoOOH from the PLNPs as a result of the reaction of AA and CoOOH (Figure 2A). Figure 2B shows the linear correlation (R = 0.9941) between the PL intensity and the AA concentrations, ranging from 1 to 100 μM. As defined by IUPAC,[26] 13 determinations were made according to the experimental method, and the standard deviation was calculated to be 0.16. The regression equation was $\Delta F = 0.8445[AA] + 12.7843$. The detection limit was calculated to be 0.59 μM. Kinetic studies showed that the nanoprobe responded rapidly to AA in an instantaneous mode (Figure S11, Supporting Information). The recovery of PL was attributed to the reduction of CoOOH to Co^{2+} by AA, leading to the separation of CoOOH from PLNPs. Figure S12 (Supporting Information) shows that an absorption peak of Co^{2+} at 510 nm appeared in the supernatant after the reaction compared with the case before the reaction. During the redox reaction, AA was oxidized to generate dehydroascorbic acid, which was confirmed by the mass spectrum (Figure S13, Supporting Information). As shown in Figure S14 (Supporting Information), the reaction

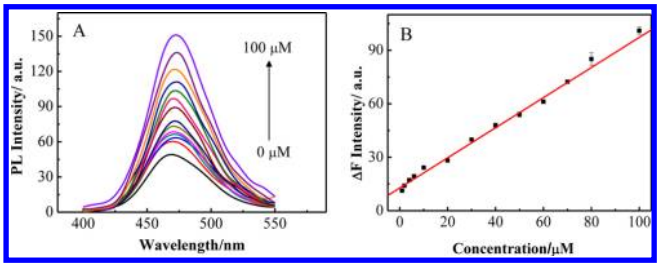

Figure 2. (A) PL emission spectra of CoOOH-modified PLNPs as a function of AA concentration (0, 1, 2, 4, 6, 10, 20, 30, 40, 50, 60, 70, 80, and 100 μM) in aqueous solution. (B) Enhanced PL intensity (ΔF) against the AA concentration over the linear range of 1−100 μM.

dx.doi.org/10.1021/ac5000587 | Anal. Chem. 2014, 86, 3924−3930

ratio of AA and CoOOH was 1:2. The reaction equation was concluded to be

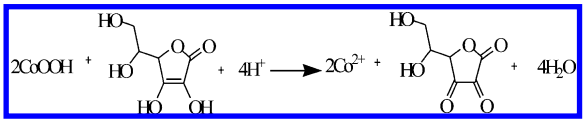

Selectivity of the Nanoprobe. The selectivity is a key property of the probe for application when used in living cells, because the activity of AA would be influenced by other reactive species existing in living cells. The selectivity of the nanoprobe toward AA has been examined by monitoring the changes in the PL intensity for the nanoprobe upon exposure to various interfering agents and AA. Notably, this response of the nanoprobe is highly selective toward AA compared with other interfering agents. The results revealed that a wide range of electrolytes and reducing compouds such as GSH and Gly did not cause obvious interference (Figure 3).

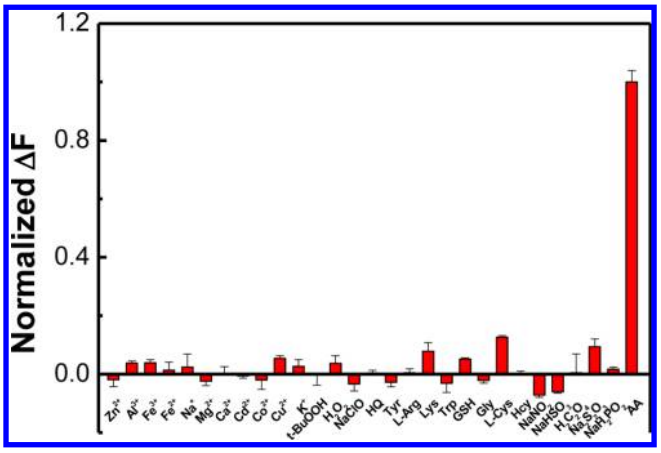

Figure 3. PL response of CoOOH-modified PLNP solutions in the presence of different electrolytes and biomolecules: AA (100 μM), Fe^{3+} (0.36 mM), Fe^{2+}(10 μM), Al^{3+}, Mg^{2+}, Na^{+}, and Zn^{2+} (0.18 mM), Cu^{2+}, K^{+}, and Ca^{2+} (0.12 mM), Cd^{2+} (36 μM), Co^{2+} (0.36 mM), NaClO (1.2 mM), H_2O_2 (10 μM), t-BuOOH and hydroquinone (HQ) (36 μM), GSH (1 mM), L-Cys (100 μM), Tyr, L-Arg, Lys, Gly, Hcy, and Trp (10 μM), $NaHSO_3$ and NaH_2PO_2 (100 μM), $H_2C_2O_4$ and $NaNO_2$ (500 μM), $Na_2S_2O_3$ (1 mM).

Detection of AA in Cell Extracts. The nanoprobe was then applied to detect AA in cell extracts. At first, the signal and background of the cell extract solution with and without in situ excitation were recorded. The cell extract solution without the probe generated a strong fluorescent background under 365 nm excitation (Figure 4A). To avoid the fluorescent background noise generated from in situ excitation, the cell extract solution with the nanoprobe was irradiated for 10 min before detection, avoiding further excitation during the detection process. In this case, the signal-to-noise ratio was greatly improved (Figure 4B). The results suggested that the long-lasting PL detection using the nanoprobe could effectively eliminate autofluorescence and scattering of light from biological matrixes encountered under in situ excitation. As shown in Figure 4C, the cell extract solution with PLNPs exhibited bright blue long-lasting PL (sample a), while the cell extract solution with the nanoprobe showed a dark view (samples b and c), indicating that the PL of PLNPs was efficiently quenched by CoOOH. When a proper amount of AA was added to sample c, the cell extract solution showed bright blue long-lasting PL (Figure 4D), suggesting that the nanoprobe could be successfully employed to detect

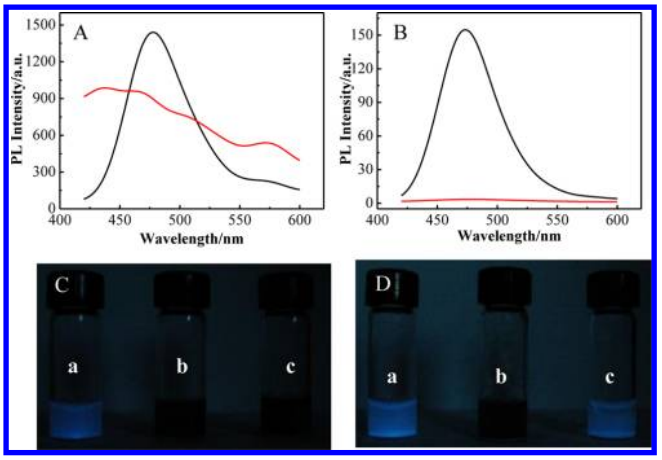

Figure 4. PL spectra of cell extract solutions with detectable AA (100 μM) in the absence (red line) or presence (black line) of the nanoprobe: (A) under in situ excitation (365 nm); (B) upon removal of the excitation source after excitation using a UV lamp for 10 min. (C) Photographs of the cell extract solution with PLNPs (a) and the nanoprobe (b, c) in the dark. (D) Photographs of the cell extract solution with PLNPs (a), the nanoprobe (b), and the nanoprobe and AA (c) in the dark. The samples were excited with a UV lamp for 10 min before the photographs were taken in the dark.

AA in cell extracts using its long-lasting afterglow nature. Then the detection range and the detection limit of AA in the cell extract were investigated. As shown in Figure S15 (Supporting Information), the detection range was 2.5−100 μM (the linear correlation R was 0.9968) in the cell extracts. The detection limit was calculated to be 2.20 μM according to the method mentioned above.

Persistent Luminescence Imaging of the Nanoprobe in Living Cells. We next sought to apply the nanoprobe for detection and imaging of AA in living cells. The nanoprobe (0.2 mg/mL) was incubated with RAW 264.7 macrophages for 1 h at 37 °C. The sample was excited with a UV lamp before the imaging experiments. The nanoprobe was no longer excited during the whole imaging process to avoid autofluorescence and scattering of light from the living cells. Negligibly weak PL was observed after incubation of the nanoprobe with RAW 264.7 macrophages (Figure 5A). However, Figure 5B shows

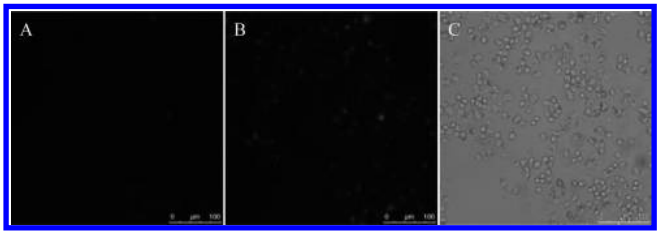

Figure 5. PL imaging of AA in living cells. (A) PL image of the nanoprobe in RAW 264.7 macrophages. (B) PL image of the same sample after the addition of AA (100 μM). (C) Bright-field image of the samples in (A) and (B). Scale bars are 100 μm.

observable PL after the addition of AA in the same sample, demonstrating that the nanoprobe could detect and image AA in living cells without excitation. The bright-field image (Figure 5C) confirmed that the cells were viable throughout the imaging experiments.

MTT Assay. To evaluate the cytotoxicity of the nanoprobe, we performed an MTT assay in RAW 264.7 macrophages with

dx.doi.org/10.1021/ac5000587 | Anal. Chem. 2014, 86, 3924−3930

different nanoprobe concentrations (0, 0.2, 0.5, 1.0, 1.5, and 2.0 mg/mL). The absorbance of MTT at 490 nm is dependent on the degree of activation of the cells. Then the cell viability was expressed by the ratio of the absorbance of the cells incubated with the nanoprobe to that of the cells incubated with culture medium only. Figure S16 (Supporting Information) shows that the cell viability was more than 90% when the concentration of the nanoprobe was up to 2.0 mg/mL, indicating that the nanoprobe exhibited low cytotoxicity in the living cells.

Persistent Luminescence Imaging of the Nanoprobe in Vivo. We next assessed the ability of the nanoprobe to image AA in a mouse model. Two Kunming mice were chosen for the nanoprobe. One mouse (the left one in both panels in Figure 6) was injected with 0.1 mL of normal saline, and another (the right one in both panels Figure 6) was injected with 0.1 mL of AA solution. Then 0.1 mL of CoOOH-modified PLNPs (1 mg/mL, excited by a 365 nm UV lamp for 10 min before injection) was injected at the same site as above for the two mice. The PL of the nanoprobe was collected immediately without excitation. As shown in Figure 6A, the mouse treated

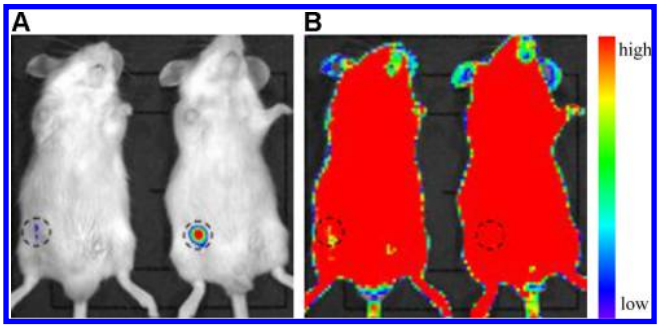

Figure 6. PL imaging of AA in vivo. (A) PL image of the mouse treated with 0.1 mL of normal saline and the nanoprobe (left) and the mouse treated with 0.1 mL of AA (0.1 mol/L) and the nanoprobe (right) without excitation. (B) PL image of the same mice in (A) using 420 nm excitation. The concentration of the nanoprobe was 1 mg/mL. The PL signals were collected at 520 ± 20 nm. The center of the black dashed circle is the injection site. The color change from purple to red for the intensity bar represents the increase in the luminescence intensity.

with normal saline and the nanoprobe did not show obvious fluorescence, while the mouse treated with AA and the nanoprobe showed strong fluorescence under the same conditions. The result was consistent with the imaging results in living cells, which indicated that the nanoprobe was capable of detecting AA in vivo. However, the PL signals were sheltered by the background noise for the same mice when 420 nm excitation (Figure 6B) was used. The results revealed that the current nanoprobe could effectively avoid autofluorescence and scattering of light from biological samples under in situ excitation.

CONCLUSION

In summary, we have demonstrated a novel nanoprobe, based on the specific reaction of CoOOH and AA, that can detect and image AA in living cells and in vivo. PLNPs were employed as the photoluminescence unit, and CoOOH nanoflakes were used as the quencher. The CoOOH-induced quenching effect can be reversed in the presence of AA, thereby enabling the highly selective and instantaneous detection of AA. Moreover, detection and imaging of AA in living cells and in vivo without external excitation can be achieved because of the long-lasting afterglow nature, which allows the removal of autofluorescence and scattering of light from biological matrixes produced by in situ excitation. We anticipate that this approach provides new insights for monitoring reactive species in living cells and in vivo.

ASSOCIATED CONTENT

Supporting Information

Supporting figures as noted in text. This material is available free of charge via the Internet at http://pubs.acs.org.

AUTHOR INFORMATION

Corresponding Author

*E-mail: tangb@sdnu.edu.cn.

Notes

The authors declare no competing financial interest.

ACKNOWLEDGMENTS

This work was supported by the 973 Program (Grant 2013CB933800), National Natural Science Foundation of China (Grants 21227005, 21390411, 91313302, 21035003, 21375081, and 21105059), and Program for Changjiang Scholars and Innovative Research Team in University.

REFERENCES

(1) Finkel, T.; Holbrook, N. J. *Nature* **2000**, *408*, 239−247.
(2) Seitz, H. K.; Stickel, F. *Nat. Rev. Cancer* **2007**, *7*, 599−612.
(3) Wilson, W. R.; Hay, M. P. *Nat. Rev. Cancer* **2011**, *11*, 393−410.
(4) Ueno, T.; Nagano, T. *Nat. Methods* **2011**, *8*, 642−645.
(5) Chan, J.; Dodani, S. C.; Chang, C. J. *Nat. Chem.* **2012**, *4*, 973−984.
(6) Yang, Y.; Zhao, Q.; Feng, W.; Li, F. *Chem. Rev.* **2013**, *113*, 192−270.
(7) Koide, Y.; Urano, Y.; Hanaoka, K.; Terai, T.; Nagano, T. *J. Am. Chem. Soc.* **2011**, *133*, 5680−5682.
(8) Dickinson, B. C.; Lin, V. S.; Chang, C. J. *Nat. Protoc.* **2013**, *8*, 1249−1259.
(9) Zhang, W.; Li, P.; Yang, F.; Hu, X.; Sun, C.; Zhang, W.; Chen, D.; Tang, B. *J. Am. Chem. Soc.* **2013**, *135*, 14956−14959.
(10) Resch-Genger, U.; Grabolle, M.; Cavaliere-Jaricot, S.; Nitschke, R.; Nann, T. *Nat. Methods* **2008**, *5*, 763−775.
(11) Lavis, L. D.; Raines, R. T. *ACS Chem. Biol.* **2008**, *3*, 142−155.
(12) Deng, R.; Xie, X.; Vendrell, M.; Chang, Y. T.; Liu, X. *J. Am. Chem. Soc.* **2011**, *133*, 20168−20171.
(13) Xiong, B.; Zhou, R.; Hao, J.; Jia, Y.; He, Y.; Yeung, E. S. *Nat. Commun.* **2013**, *4*, 1708.
(14) Jaffe, G. M. *Handbook of Vitamins*; Marcel Dekker: New York, 1984; pp 199−244.
(15) Carr, A. C.; Frei, B. *Am. J. Clin. Nutr.* **1999**, *69*, 1086−1107.
(16) Chen, Q.; Espey, M. G.; Sun, A. Y.; Pooput, C.; Kirk, K. L.; Krishna, M. C.; Khosh, D. B.; Drisko, J.; Levine, M. *Proc. Natl. Acad. Sci. U.S.A.* **2008**, *105*, 11105−11109.
(17) Enstrom, J. E. *Vitamin C in Health and Disease*; Marcel Dekker: New York, 1997; pp 381−398.
(18) Padayatty, S. J.; Riordan, H. D.; Hewitt, S. M.; Katz, A.; Hoffer, L. J.; Levine, M. *Can. Med. Assoc. J.* **2006**, *174*, 937−942.
(19) Esteban, M. A.; Pei, D. *Nat. Genet.* **2012**, *44*, 366−367.
(20) Le Masne de Chermont, Q.; Chaneac, C.; Seguin, J.; Pelle, F.; Maitrejean, S.; Jolivet, J. P.; Gourier, D.; Bessodes, M.; Scherman, D. *Proc. Natl. Acad. Sci. U.S.A.* **2007**, *104*, 9266−9271.
(21) Wu, B.-Y.; Wang, H.-F.; Chen, J.-T.; Yan, X.-P. *J. Am. Chem. Soc.* **2011**, *133*, 686−688.
(22) Maldiney, T.; Lecointre, A.; Viana, B.; Bessière, A.; Bessodes, M.; Gourier, D.; Richard, C.; Scherman, D. *J. Am. Chem. Soc.* **2011**, *133*, 11810−11815.

(23) Pan, Z.; Lu, Y.-Y.; Liu, F. *Nat. Mater.* **2012**, *11*, 58−63.
(24) Wu, Q. D.; Gao, X. P.; Li, G. R.; Pan, G. L.; Yan, T. Y.; Zhu, H. Y. *J. Phys. Chem. C* **2007**, *111*, 17082−17087.
(25) Jagadale, A. D.; Dubal, D. P.; Lokhande, C. D. *Mater. Res. Bull.* **2012**, *47*, 672−676.
(26) Irving, M. N. H.; Freiserand, H.; West, T. S. *IUPAC Compendium of Analytical Nomenclature Definitive Rules*; Pergamon Press: Oxford, U.K., 1978.